



## Analysis the Linear Optical Constant of Lanthanum Doped Nickel Ferrites Nanoparticles from Absorption Spectra

**Sai Krishna Dhanush Jakku**

Dept. of ECE, Aditya Engineering College, Surampalem, A.P., India  
[jakkusaikrishnadhanush@gmail.com](mailto:jakkusaikrishnadhanush@gmail.com)

**Surya Priya Mada**

Dept. of ECE, Aditya Engineering College, Surampalem, A.P., India  
[madasuryapriya@gmail.com](mailto:madasuryapriya@gmail.com)

**Venkata Sai Nathi**

Dept. of ECE, Aditya Engineering College, Surampalem, A.P., India  
[venkatasai7@gmail.com](mailto:venkatasai7@gmail.com)

**Dr. N. R. Dhineshababu**

Professor, Dept. of ECE, Aditya Engineering College, Surampalem, A.P., India  
[dhineshababu@aec.edu.in](mailto:dhineshababu@aec.edu.in)

### Abstract

Due to their optical properties, which are also essential in the creation of devices employed in the optoelectronic and photonic domains, several nanomaterials are quite fascinating. The scientific community wants to know more about the physical processes that underlie these nanomaterials. In this study, Nickel Ferrites (NiFe<sub>2</sub>O<sub>4</sub>) nanoparticles (NPs) were prepared via co-precipitation, and the precise optical characteristics of the nanoparticles were assessed using UV-Vis spectroscopy. The samples were described using scanning electron microscopy, structural and phase purity analysis (X-ray diffraction), and morphological examination. To analyze the particle size distribution and UV absorption spectra, the spherical La doped NiFe<sub>2</sub>O<sub>4</sub> nanoparticles were dispersed in water at a frequency of 25 kHz. Using these absorption spectra, we subsequently investigated La doped NiFe<sub>2</sub>O<sub>4</sub> nanoparticles to see if they may serve as a material for solar cells, biomedicine, wastewater treatment, catalysis, and electronic devices. Applications for optoelectronic devices could make use of these findings.

**Keywords:** Nickel Ferrite Nanoparticles, Co-precipitation, Scanning electron microscopy, UV-Vis spectroscopy, X-ray diffraction, UV absorption spectra, Optical Properties.

### Introduction

We have advanced to a new level of understanding mainly because of numerous new developments in Nano science around the world that combine physics, chemistry, material science, and biosciences. Science fiction heavily depends on nanotechnology, which synthesize nanoparticles (NPs) on a nanometer scale. Spinel ferrite (MFe<sub>2</sub>O<sub>4</sub>), the most extensively correlated spinel oxide among the several categorized ferrite materials, has a variety of optical, electrical, magnetic, and electronics transport properties. For application at microwave frequencies, their high electrical resistivity and minimal

eddy current losses make them the ideal material.

The amazing features of the nanoscale spinel ferrites make them particularly useful in the field of material research. Ni spinal Fe has been prepared using a variety of techniques so far, including solid state, sol-gel, ball-milling, co-precipitation, and micro-emulsion, and others. Large magnetic moments and luminous characteristics of rare earth ions have a significant impact on the crystal properties.

Strong rare earth permanent magnets are used as electrical insulators and in a variety of electro-mechanical systems for substantial industrial applications. Lanthanum (La) ions,

chemically stable photo-luminescent materials, are another fascinating possibility. They are employed to create an infrared-absorbing glass that is used in catalytic, biomedical, electrode, carbon lighting, and water treatment applications due to their high refractive index and low dispersion indices. Attempts have been made to study the La-doped ferrites such as Manganese, nickel, copper, and cobalt. In this study, NiFe<sub>2</sub>O<sub>4</sub> NPs were synthesized by co-precipitation method. The doped ion of La (50%) was added to NiFe<sub>2</sub>O<sub>4</sub> NPs in the same preparation route. The optical characteristics of the NPs were later determined.

### • Co – Precipitation Method

Co-precipitation reactions occur when nucleation, growth, coarsening, and/or agglomeration activities take place at the same time. Co-precipitation responses display the following traits:

- The products are often insoluble species that are generated under highly saturated environments.
- The formation of many tiny particles during nucleation is a crucial stage.
- Secondary processes that alter the size, shape, and characteristics of the products significantly include aggregation and Ostwald ripening.

Typical synthetic co - precipitation methods include:

- Metals synthesized from aqueous solutions via electrochemical reduction, reduction from non-aqueous solutions, and breakdown of metallorganic precursors.
- Both aqueous and non-aqueous solutions can produce oxides.
- Metal chalconides produced via molecular precursor processes.
- Co-precipitation aided by a microwave or sonication.

The co-precipitation approach has a few benefits:

- Easy and quick preparation.
- Simple control over particle structure and size.
- The surface state and overall

homogeneity of the particle can be changed in a number of ways.

- Moderate temperature.
- Energy effective.
- No use of an organic solvent at all.

Negative aspects include:

- Not applicable to species without charges.
- Traces of contaminants may precipitate with the product.
- Takes a lot of time.
- Issues with reproducibility from batch to batch.
- If the reactants have significantly varied rates of precipitation, this approach does not perform effectively.

### • Photoluminescence

Photoluminescence is a process that allows any kind of material to generate light (electromagnetic radiation). The energy of the stimulating photon in relation to the emission is one of many factors that can be used to categorize photoluminescence processes. A scenario known as resonance excitation occurs when photons of a specific wavelength are absorbed and then rapidly reemitted at a different wavelength. Resonance fluorescence is a common name for this. This process involves electrons for materials in solution or the gas phase, but there are no substantial internal energy changes involving the chemical substance's molecular components between absorption and emission. Photoluminescence (PL) is the term for the spontaneous light emission that occurs when a substance is excited optically. The excitation energy and intensity are chosen to test different sample locations and excitation concentrations. Through PL research, a variety of material parameters can be described. PL spectroscopy, which is also a very sensitive and selective probe of discrete electronic states, offers electrical (as opposed to mechanical) characterization. The emission spectrum's characteristics can be utilized to determine the levels of surfaces, interfaces, and impurities as well as to assess alloy disorder and interface roughness.

- Optical Properties

Optical characteristics are useful to determine how a material interacts with light. The optical properties of matter are examined in optical physics, a subfield of optics. Optical properties of matter include:

- Refractive index
- Dispersion
- Transmittance and transmission coefficient
- Absorption
- Scattering
- Turbidity
- Reflection and reflectivity (reflection coefficient)
- Fluorescence
- Phosphorescence
- Photoluminescence
- Optical bistability
- Photosensitivity

are just a few of the variables that are considered. The area of physics known as optics studies how light behaves and how it interacts with materials. The term "light" refers to an electromagnetic radiation type that makes objects visible or allows the human eye to see them. It can also be described as radiation that can be seen with the naked eye. The behavior of ultraviolet, visible, and infrared light is described by optics.

## II. LITERATURE REVIEW

[1] N. R. Dhineshabu et al. recommended that copper spinel ferrites ( $\text{CuFe}_2\text{O}_4$  and lanthanum-doped  $\text{CuFe}_2\text{O}_4$  nanoparticles) were produced using the sol-gel technique. Both spinel ferrite nanoparticles' absorption spectra were used to further analyse their refractive index, optical conductivity, absorption coefficient, band gap energy, extinction coefficient, dielectric tangent loss, dielectric constant, and Urbach energy. La-doped  $\text{CuFe}_2\text{O}_4$  nanoparticles can be exploited in optoelectronics applications, according to the optical investigations.

[2] N. R. Dhineshabu and R. Vettumperumal expressed that different nanomaterials are extremely intriguing due to their optical properties, which are also crucial in the creation of devices used in the optoelectronic and photonic domains. The scientific

community is interested in learning more about the physical processes that underlie these nanomaterials. Using a sonochemical approach, copper oxide ( $\text{CuO}$ ) nanoparticles (NPs) were created in this study, and UV-Vis spectroscopy was used to analyse their precise optical characteristics. The Wemple-DiDomenico single-oscillator method was used to determine the oscillator strength, static refractive index, dispersion energy ( $E_d$ ), energy of effective dispersion oscillator ( $E_o$ ), carrier concentration, and  $N/m^*$  values in order to depict the normal dispersion of the refractive index of the  $\text{CuO}$  NPs. The refractive index, third-order nonlinear susceptibility, and optical polarization were other nonlinear optical properties that were estimated. Using optiFDTD software, the nonlinear optical performance of the  $\text{CuO}$  NPs was simulated, and the nonlinear output power, spectral bandwidth, and acceptance angle were determined. Applications for optoelectronic devices could make use of the findings.

[3] A Berry et al. projected that for Dense Wavelength Division Multiplexing (DWDM) applications, a photonic crystal ring resonator (PCRR)-based optical demultiplexer is reported. An eight-channel PCRR can develop and simulate materials like diamond and silicon dioxide. For the proposed demultiplexer, using silicon-dioxide and diamond, respectively, an average uniform spacing of 0.8 nm and 1.94 nm is attained. A maximum transmission efficiency of 91.48% is achieved by silicon dioxide for the eight-channel PCRR configuration. 1613.333 is the quality factor value. The ring resonator is discovered to be the most convenient and ideal among the several optical devices available based on photonic crystals for dense wavelength division multiplexing due to its light guiding mechanism.

[4] A Garhwal et al. impelled that distributed sensors for the electron cloud are proposed with a tiny Sagnac interferometer integration. The Sagnac interferometer is made up of a Sagnac loop and four microring probes. To create the plasmonic wave oscillation, the silver bars are placed in each of the microring probes. In the central microrings, where the plasmonic antennae are set up and used for

wireless fidelity (WiFi) and light fidelity (LiFi) transmissions for distributed sensors, electrons are trapped and oscillated by whispering gallery modes (WGMs). The four antennas that are generated at the centre microrings have corresponding antenna gains of 2.59dB, 0.93dB, 1.75dB, and 1.16dB. The interferometer input receives 1.50  $\mu$ m wavelength polarized light that has been randomly polarized in upstream and downstream directions. The space-time modulation control can be used to acquire the polarization components. The space-time projection can be used to achieve the ultra-high measurement resolution in terms of quick switching times (changes in phase) by manipulating the spin orientation of the electron cloud. In manipulation, a change in the input source's power replaces the applied stimulus. Changes in light input power lead to variations in electron cloud density. Similar to this, the microscopic media, which can be used as microscopic sensors, excites the electron cloud.

[5] A Muralidharan et al. proposed that one of the fundamental combinational logics utilized in digital electronic circuits is the usage of digital comparators. These standard devices are constructed with CMOS transistors and copper interconnects. With transistor sizes dropping to as low as 7 nanometers, CMOS technology is almost at its limit. Optical combinational and sequential circuit design has made use of micro-ring resonators (MRR). The design and simulation of an all-optical magnitude comparator using two separate light wavelengths with the same or different amplitude values and delivered to a dual micro-ring resonator are presented in this study. The outcomes of the comparison depend on the outputs' position and intensity. For a single ring resonator design with an effective refractive index of 2.285, ring resonator designs have a compact footprint of 1500  $\mu$ m<sup>2</sup> and a high quality factor of 627. The FWHM and FSR measurements are 5.07 nm and 33.34 nm, respectively. These gadgets can function at frequencies as high as 1.6 THz. The propagation delay, in contrast to typical devices, is only 640 fs.

[6] A Warren et al. introduced that in this study, we investigate the potential benefits of nano-structure arrays for plasmonic sensors and imaging technology. In comparison to devices based on individual structures, the range of parameters that can be changed to produce a particular response rises substantially when utilizing a periodic array. We demonstrate that plasmonic arrays can be designed to exhibit high-quality spectrum extinction peaks that are predominantly influenced by the angle of incidence and period with little structural dependence. This provides design freedom for plasmonic sensing or imaging equipment. Both the creation of the nanostructure arrays and the visual confirmation of the localized plasmon resonance response are discussed. Utilizing the software Scattering by Multiple Particles in Thin Film Systems (SMUTHI), which is beneficial for analysing the response of plasmonic arrays, spectral simulation results are also produced for the arrays.

[7] AE Arumona et al. suggested that for ultra-high density up- and downlink transmission, a novel device is suggested. The instrument consists of a panda ring resonator with silver bars in the center and chalcogenide Mach-Zehnder interferometer (MZI) with upper and lower portions. The device's operation relies on a space-time function, in which the input space (soliton) is multiplexed with time at the add port using a wavelength bandwidth of 1.50-3.50  $\mu$ m and a frequency bandwidth of 85-250 THz. With the proper parameters, the WGM may be seen at the upper (uplink) and lower (downlink) center microrings. The uplink and downlink plasmonic antennas have directivity of 18.68 and 13.27, and gains of 9.34 and 6.64, respectively, are formed by the silver bars at the central microring. While wireless fidelity (WiFi uplink and downlink) uses the frequency spectrum, light fidelity (LiFi uplink and downlink) makes use of the wavelength spectrum. While the WiFi uplink and downlink operate best at frequencies of 130 THz and 132 THz, the LiFi uplink and downlink operate best at wavelengths of 2.30  $\mu$ m and 2.27  $\mu$ m, respectively. The bit rate for the transmission signal is 28 Pbits/one. The system performance is shown by the bit error

rate (BER) value of 0.36. High system performance is indicated by a low BER value. The gadget can be used for 6G communication's coverage of the light-wave and microwave bands, enabling the use of artificial intelligence (AI), 3D communication, code encryption, and secured transmission.

[8] IS Amiri et al. postulated that the silicon microring resonator arrangement is proposed for use with the Frequency Shift Keying (FSK) dual-transmission method for short-range communication. Using three more microring resonators and an optically modified add-drop multiplexer with a gold grating inserted in it, FSK is produced. A transmitted microring with two nano-ring phase modulators connected to a receiver via a 10 km fiber channel makes up the proposed system. Three corresponding microring systems make up the user end. Each sensor probe is identified by the Bragg wavelength thanks to a gold grating that is inserted in the center of the two side rings (the sensor probes) to introduce the plasmonic polariton. The Whispering Gallery Mode (WGM), which is caused by light propagation, can be achieved by managing the employed two sides smaller ring resonator in the proposed ring structures. The frequency of the  $n$  photonic oscillator is in the range of plasmonic frequencies. Another form of transmission known as light fidelity (LiFi) transmission can be employed with the WGM beam. The 1.55  $\mu\text{m}$  wavelength of the FSK light source was fed into the system during manipulation. 200 Tbits/s of transmission bit rates are attained. With more input power, the Bit Error Rate (BER) measured at the user ends rises. The Bragg wavelength was determined by each sensor node, and the change in Bragg wavelength was measured on each sensor and proven to have a linear trend, which is helpful for sensing applications. The suggested system can transmit data wirelessly or over cable depending on the application, however in this case, cable-based LiFi is more dependable than WiFi in terms of security, effectiveness, availability, and safety.

[9] A Garhwal et al. impelled that for applications involving plasma sources, a microring circuit employing space-time distortion control is suggested. The microring

circuit is made up of a small ring in the center and two smaller rings on either side. A metallic layer is inserted within the central microring circuit. The circuit is subjected to space-time management, and the resonant optical path difference of the two-side rings is used to accomplish the least amount of space-time distortion. By matching the space-time distortion in terms of the optical path difference, the whispering gallery mode (WGM) is created. The trapped electron cloud oscillation is brought about by the interaction of the WGM and electrons on the metallic film surface. The plasmonic wave oscillation, which produces the electron cloud's plasma frequency, allows for the calculation and measurement of the plasma force. Applications such as dry spray, force sensors, and electron cloud speed involve the investigation of the plasma force produced by particular metallic coatings. The simulation results produced have revealed that the plasma frequencies of  $1.93 \times 10^{16}$ ,  $1.91 \times 10^{16}$ , and  $1.88 \times 10^{16}$  rad/s are obtained for gold, silver, and copper films, respectively. These frequencies were reached by applying the practical device parameters. Calculations are made regarding the electron cloud plasma speed and force sensor sensitivity.

[10] A Shaikh et al. expressed that the proposed work entails the creation of an algorithm and computer simulation of a photonic sensor based on a hexagonal ring structure for the identification of dangerous water contaminants. Lead, DDT, Chlorine, PCB, Arsenic, Mercury, Fluoride, and Aluminum impurities are among those that can be found using an optical sensor ring construction. For various water contaminants, a comparison between two types of sensor structures is looked into. The developed optical sensor, which has an output value of 0.4 and provides quick, accurate output, is seen to have a higher amplitude fluctuation, for instance 1.7 for lead contaminants. For the created sensing sensor, a sensitivity of 350 nm/RIU and a Q factor of 3453 are obtained. The outcome has demonstrated a realizable fabrication option for sensing applications in the future. The work done has a lot of promise

for use in detecting contaminants in drinking water applications.

## MATERIALS AND CHARACTERIZATION

### • Materials

The selected precursors, from Merck, were lanthanum nitrate ( $\text{La}(\text{NO}_3)_3 \cdot 6\text{H}_2\text{O}$ , 99%); nickel nitrate hexahydrate ( $\text{NiNO}_2\text{O}_6 \cdot 3\text{H}_2\text{O}$ ; 99%); ferric nitrate nanohydrate ( $\text{Fe}(\text{NO}_3)_3 \cdot 9\text{H}_2\text{O}$ ; 99%); and sodium hydroxide ( $\text{NaOH}$ , 98%). Double-distilled water was used without further purification.

### • Characterization

By using the powder X-ray diffraction pattern, the synthesized Nano ferrites phase was determined (XRD, Philips PW-1830).

The surface morphology of the samples was examined using a scanning electron microscope (SEM; JSM6700F; JEOL, USA). The La doped  $\text{NiFe}_2\text{O}_4$  nanoparticles were disseminated in water solution at a ratio of 1:100 and maintained under ultrasonic irradiation (25 kHz) to create a homogenous mixed solution. Utilizing a particle size analyzer (PSA; Nanophox, Germany) and a UV spectrophotometer (Lamda 20; PerkinElmer), this solution was utilized to examine the particle size distribution using a dynamic light scattering technique.

## III. METHODOLOGY

Nanoparticles of nickel ferrite ( $\text{NiFe}_2\text{O}_4$ ) were created using the co-precipitation process. In this procedure, the stoichiometric amounts of ferric nitrate nanohydrate ( $\text{Fe}(\text{NO}_3)_3 \cdot 9\text{H}_2\text{O}$ ) and nickel nitrate hexahydrate ( $\text{NiNO}_2\text{O}_6 \cdot 3\text{H}_2\text{O}$ ) are separately added to the sodium hydroxide ( $\text{NaOH}$ ) solution.



The pH of the mixture was continuously checked as the  $\text{NaOH}$  solution was added drop by drop. The reactants were continuously mixed with a magnetic stirrer until pH 12 was

achieved. Oleic acid was included into the mixture in a pre-set amount as the surfactant.

Once heated to  $80^\circ\text{C}$ , the liquid precipitate was agitated for 40 minutes. The product was cooled to room temperature (precipitation), and the sample needs to be washed twice with distilled water and ethanol (filter) to remove any undesired impurities and the leftover surfactant from the prepared sample. The material was then dried overnight at a temperature of about  $80^\circ\text{C}$  after being centrifuged. The purchased material was subsequently processed into a fine powder.

**Precipitation:** Chemical precipitation is the most widely used method for removing dissolved (ionic) metals from solutions, such as process wastewaters containing dangerous metals. The ionic metals are changed into an insoluble form (particle) via a chemical reaction between the soluble metal compounds and the precipitating agent. The particles created by this reaction are removed from the solution using filtration.

**Filtration:** Filtration is the act of removing suspended solids from a liquid by allowing the liquid to flow through the pores of a membrane known as a filter. Nanofiltration, a membrane filtration-based method, is a technique in which the particles smaller than 10 nanometers can flow through the membrane through nanometer-sized pores used in nanofiltration. Nanofiltration membranes have pores that are 1 to 10 nanometers in size, which makes them slightly larger than reverse osmosis membranes but smaller than microfiltration and ultrafiltration membranes. Thin polymer films are the most typical material used to create membranes.

Finally, the results of the optical properties of Nickel Ferrite nanoparticles are characterized with XRD, SEM, UV spectroscopy, Optical Band gap and some studies.

## IV. RESULTS

### • Scanning Electron Microscopy

A picture of the sample is created by scanning the surface with a focussed electron beam in a

scanning electron microscope (SEM). Presented in the figure is a SEM image of the nanoferrites at room temperature. Images captured by a SEM were utilized to investigate the nanoferrites' morphology. It is abundantly obvious from the photographs that the synthesized ferrites are spherical and heavily agglomerated. The high surface and dangling bonds of the nanoferrites are what causes agglomeration at nano-level. Agglomeration occurs in the nanoferrite samples because the atoms in the nanoferrites try to form bonds, and these bonds then try to form bonds between the adjacent particles. The figure illustrates that the particles are nano-sized and their uneven/irregular distribution, and it was discovered that the synthesized La doped NiFe<sub>2</sub>O<sub>4</sub> nanoferrites had particles that ranged in size from 20 to 90 nm.

#### • Particle Size Distribution

The percentage of particles of a particular size (or in a certain size interval) is shown by the particle size distribution.

Between 35 and 125 nm, La doped NiFe<sub>2</sub>O<sub>4</sub> nanoparticles are dispersed. However, the nanoparticles' average distribution (d<sub>50</sub>) is 57 nm.

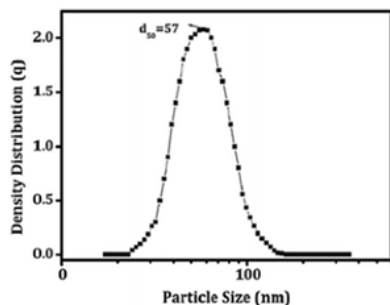
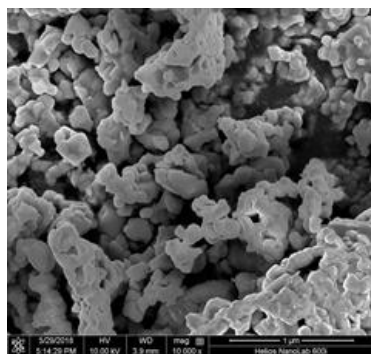


Fig: SEM image of nano ferrites at room temperature

#### • XRD Analysis

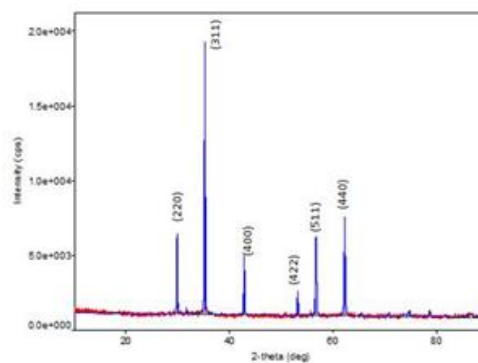
Utilizing an X-ray diffractometer (Smart Lab; Rigaku, USA) with a scan range of 10° < 2θ < 90°, the structural and phase purity of La doped NiFe<sub>2</sub>O<sub>4</sub> nanoparticles were ascertained. The figure illustrates the X-ray diffraction patterns of a rare earth (La<sup>3+</sup>) doped nickel ferrite nanocrystal synthesized by co-precipitation at calcination temperatures.

The six relevant peaks in phase analysis (220), (311), (400), (422), (511) and (440) matched well with the normal JCPDS file number (74-2081). The poly-crystalline character of the nanocrystals is shown by the X-ray diffractogram. The mean crystallite size was calculated from the highest typical peak (311) using Scherrer's equation as follows:

where D is the mean crystallite size (nm), λ = 1.54178 Å is the X-ray wavelength, k = 0.89 (approx.) which is the crystallite-shape factor, β is the full width at half maximum and θ is the Bragg angle. Crystalline size is 11.14 nm on average.

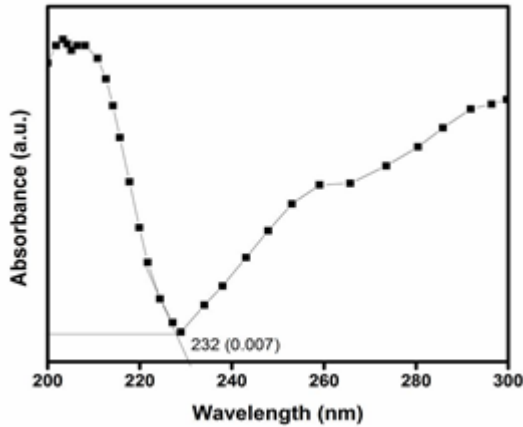
$$D = \frac{k\lambda}{\beta \cos \theta}$$

#### • UV Spectroscopy



UV spectra were examined for the prepared La doped NiFe<sub>2</sub>O<sub>4</sub> nanoparticles in order to assess the optical property. When it comes to analyzing the optical characteristics of powdered nanoferrites, the DRS spectrum offers an edge over UV-Vis absorption spectroscopy.

The optical bandgap energy ( $E_g$ ) is calculated from the manufactured nanoferrites' absorption spectral curve by extrapolating through the wavelength axis, as shown in the figure.

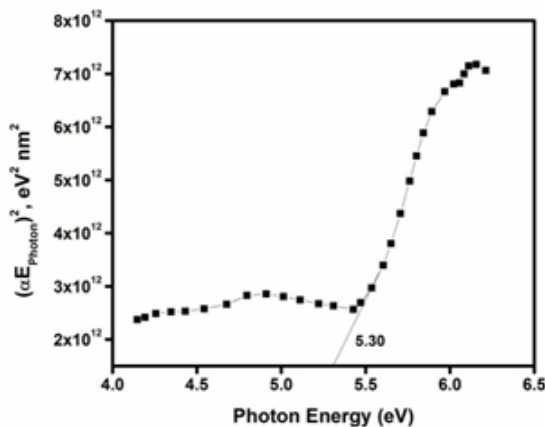


The absorbance is 0.007 and the absorption value is 232 nm. The direct and indirect bandgap energies of nanoferrites were determined using the following equation, which is connected to photon energy and absorbance.

• Direct Band Gap

Bandgap is a term used to describe the energy difference between the valence band and the conduction band. The direct bandgap transition graph  $[(\alpha E_{\text{photon}})^2 \text{ vs. } E_{\text{photon}}]$  is shown in Figure, and the bandgap value is 5.30.

The results show that the different electron momentums occurring in the bandgap energy cause a variance in the direct bandgap.



transition. These findings suggest that microwave frequency applications can make use of the manufactured nanoferrites.

where  $h$  is the Planck constant;  $\nu$  is the frequency;  $\alpha$  is the absorbance;  $\lambda$  is the wavelength of nanoferrites; and  $n$  is the electronic transition type.

$$E_{\text{gap}} = h\nu/\lambda$$

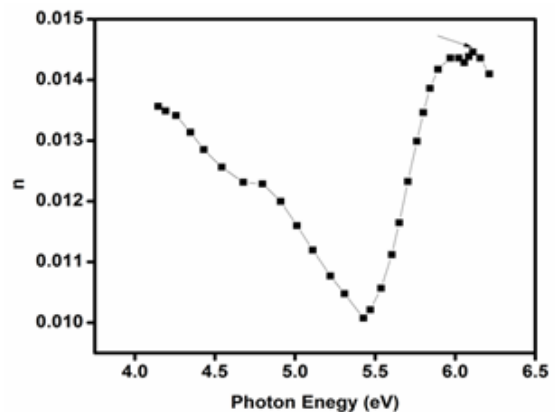
$$h\nu\alpha \propto (h\nu - E_{\text{gap}})^n$$

• Optical constants

When light strikes a material, the refractive index ( $n$ ) and extinction coefficient ( $k$ ), which are linked to refraction and absorption, respectively, determine how the material responds to the light. They may be thought of as the "fingerprint of the substance."

Refractive Index: The band gap region, for instance, has refractive index values of 0.0144. The refractive index of a semiconductor, in general, is a measurement of how transparent the semiconductor is to incident spectral radiation.

For applications in integrated optic devices, it is especially crucial to evaluate the optical material's refractive index.

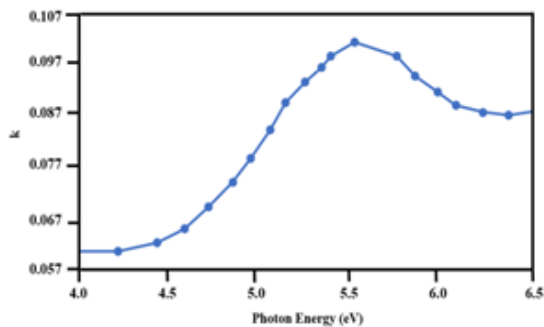




Basic Formula:  $R=1-(A+T)$ ;  $T=(1/10^A)$

Here, R- Reflectance; T- Transmittance; A- Absorption.

**Extinction Coefficient:** The extinction coefficient is a characteristic that describes how strongly a species absorbs or reflects radiation or light at a certain wavelength. The extinction coefficient of La doped NiFe<sub>2</sub>O<sub>4</sub> nanoparticles increases with photon energy. The extremely low measured extinction coefficient values (0.106) in the absorption region indicate the uniformity and smoothness of the particle surfaces.



## V. CONCLUSION

In conclusion, The co-precipitation method was successful in synthesizing the La doped NiFe<sub>2</sub>O<sub>4</sub> nanoparticles. La doped NiFe<sub>2</sub>O<sub>4</sub> was discovered to have crystallites that were 11.14 nm in size (XRD analysis).

Through micrographical analysis, distribution of spherical La doped NiFe<sub>2</sub>O<sub>4</sub> nanoparticles was analyzed. Using PSA investigations, the particle distribution's clear average size was determined to be 57 nm.

By UV absorption, the optical properties of La doped NiFe<sub>2</sub>O<sub>4</sub> nanoparticles were examined. La doped NiFe<sub>2</sub>O<sub>4</sub> nanoparticles were discovered to have a high direct band

gap. Also, through UV absorption, the extinction coefficient, optical conductivity, refractive index, and absorption coefficient were estimated.

Therefore, it can be concluded that the La doped NiFe<sub>2</sub>O<sub>4</sub> nanoparticles have a wide range of applications in semiconductors, optics, solar cells, biomedicine, wastewater treatment, catalysts, and other fields.

## VI. REFERENCES

- [1] N. R. Dhineshabu, R. Vettumperumal, A. Narendrakumar, M. Manimala, and R. Rajesh Kanna, "Optical Properties of Lanthanum-Doped Copper Spinel Ferrites Nanoparticles for Optoelectronic Applications", *Advanced Science, Engineering and Medicine* (Vol. 9, 377–383 (7), 2017).
- [2] N. R. Dhineshabu and R. Vettumperumal, "Linear and Nonlinear Optical Properties of CuO NPs for Photonics", *Journal of Electronic Materials* (The Minerals, Metals & Materials Society 2021), <https://doi.org/10.1007/s11664-021-08901-z>
- [3] A Berry, N Anand, S Anandan and P Krishnan, "High-Performance Eight-Channel Photonic Crystal Ring Resonator-Based Optical Demultiplexer for DWDM Applications", *Plasmonics* (Springer, 2021), <https://link.springer.com/article/10.1007/s11468-021-01463-0>
- [4] A Garhwal, AE Arumona, K Ray, P Youplao, G Singh and ..., "Microring Distributed Sensors Using Electron Cloud Generated by Four-point Probe Sagnac Interferometer" (preprints.org,



2021), <https://www.preprints.org/manuscript/202102.0279>

[5] A Muralidharan, AI Rasheed and ..., "Design and Simulation of Micro-ring Resonator based Optical Comparator", 2021 2nd International ... (ieeexplore.ieee.org, 2021), <https://ieeexplore.ieee.org/abstract/document/9456294/>

[6] A Warren, M Alkaisi and C Moore, "Design of 2D Plasmonic Diffraction Gratings for Sensing and Super-Resolution Imaging Applications", 2020 IEEE International ... (ieeexplore.ieee.org, 2020), <https://ieeexplore.ieee.org/abstract/document/9129161/>

[7] AE Arumona, A Garhwal, M Bunruangsas, K Ray and ..., "Plasmonic Antenna Embedded Chalcogenide MZI Circuit for Ultra-high Density Up-and Downlink Transmission", Plasmonics (Springer, 2021), <https://link.springer.com/article/10.1007/s11468-020-01323-3>

[8] AE Arumona, IS Amiri, S Punthawanunt, K Ray and ..., "Ultra-High Capacity FSK Transmission Using Silicon Microring Embedded Gold Grating Circuits", Silicon (Springer, 2021), <https://link.springer.com/content/pdf/10.1007/s12633-020-00522-1.pdf>

[9] A Garhwal, AE Arumona, K Ray and ..., "Microplasma Source Circuit Using Microring Space-Time Distortion Control", ... on Plasma Science (ieeexplore.ieee.org, 2020), <https://ieeexplore.ieee.org/abstract/document/9194286/>

[10] A Shaikh, P Sharan, PC Srikanth and M Devi, "A novel automated framework for water impurity

detection", International Journal of ... (Springer, 2021),

<https://link.springer.com/article/10.1007/s41870-020-00601-x>

[11] A Kumari, A Pal, A Singh and S Sharma, "All-optical binary to gray code converter using non-linear material based MIM waveguide", Optik (Elsevier, 2020),

<https://www.sciencedirect.com/science/article/pii/S0030402619313476>

[12] A Carmona Valencia, "Insertion of random spaces in time domain for frequency hopping sequences for RF systems"

(repository.eafit.edu.co, 2020), <https://repository.eafit.edu.co/handle/10784/25487>

[13] A Smirnov, NW Solís Pinargote, N Peretyagin and ..., "Zirconia reduced graphene oxide nano-hybrid structure fabricated by the hydrothermal reaction method", Materials (mdpi.com, 2020), <https://www.mdpi.com/632234>

[14] AE Arumona, IS Amiri and P Yupapin, "Plasmonic micro-antenna characteristics using gold grating embedded in a panda-ring circuit", Plasmonics (Springer, 2020), <https://link.springer.com/article/10.1007/s11468-019-01031-7>